

## Three selective and sensitive “off–on” probes based on rhodamine for Fe<sup>3+</sup> imaging in living cells†

Meipan Yang, Chengchao Xu, Shaoni Li, Zhao Cheng, Jia Zhou and Bingqin Yang\*

Cite this: *RSC Adv.*, 2014, 4, 14248

Received 15th January 2014  
Accepted 18th February 2014

DOI: 10.1039/c4ra00396a

www.rsc.org/advances

Three novel rhodamine-based probes were designed and synthesized. The probes exhibited highly selective and sensitive recognition toward Fe<sup>3+</sup> over other metal ions via the rhodamine ring-opening approach, which can be used for “naked-eyes” detection. In addition, fluorescence imaging experiments of Fe<sup>3+</sup> in living cells demonstrated their valuable application in biological system.

### Introduction

As one of the most important trace element in the body, iron performs a crucial role in a wide range of biochemical processes.<sup>1–3</sup> It provides the oxygen-carrying capacity of heme and acts as a cofactor in many enzymatic reactions. Both its deficiency and overload can induce biological disorders in the living body, such as anemia, liver and kidney damage, heart failure, and diabetes.<sup>4–6</sup> Even, the cellular toxicity caused by iron ions has been linked with several serious diseases, such as Alzheimer's, Huntington's, and Parkinson's diseases.<sup>7–9</sup> Although significant contributions to the development of spectroscopic sensing for Fe<sup>3+</sup> have been made over the last few decades, there have been relatively few fluorescent probes for Fe<sup>3+</sup> which showed “off–on” signal. It might be due to its paramagnetic nature which leads to fluorescence quenching.<sup>9</sup> Therefore, the development of new Fe<sup>3+</sup> probes which exhibit fluorescence enhancement is still of great challenge and interest.

The rhodamine framework is an ideal mode to construct fluorescent probes<sup>10–20</sup> on account of its excellent photophysical properties, such as long-wavelength emission, large absorption coefficient and high fluorescence quantum yield.<sup>21</sup> Furthermore, the spirolactam ring form of rhodamine derivatives is non-fluorescent and colorless, whereas the corresponding ring-opened amide provides both chromogenic and fluorogenic responses that facilitate “naked-eyes” analyte detection. This phenomenon gives them an excellent potential for the construction of an “off–on” type fluorescent probes for Fe<sup>3+</sup>.<sup>22–25</sup> Unfortunately, most of the currently existing rhodamine-based probes for Fe<sup>3+</sup> suffered certain interferences from Cr<sup>3+</sup> and

Cu<sup>2+</sup>.<sup>26–33</sup> So the aim of recent research on probes is to expand the range of probe of high sensitivity and selectivity. Herein, we report three novel “off–on” fluorescent probes based on rhodamine B for Fe<sup>3+</sup> detection, which can be used for “naked-eyes” detection with the switch-on fluorescence and significant color changes. Moreover, the three probes can give highly selective spectroscopic responses to Fe<sup>3+</sup> over other metal ions in living cells. The probes were also characterized by X-ray crystallography, <sup>1</sup>H NMR, <sup>13</sup>C NMR spectra and mass data.

### Experimental

#### Apparatus reagents and chemicals

The fluorescence spectra were measured on a HITACHI F-4500 fluorescence spectrophotometer. Absorbance spectra measurements were performed on a Shimadzu UV-1700 spectrophotometer. NMR spectra were recorded on a Varian INOVA-400 MHz spectrometer (at 400 MHz for <sup>1</sup>H NMR and 100 MHz for <sup>13</sup>C NMR) with tetramethylsilane (TMS) as internal standard. Mass spectra were performed with Bruker micrOTOF-Q II ESI-Q-TOF LC/MS/MS Spectroscopy. IR spectra were taken in KBr disks on a Bruker Tensor 27 spectrometer. X-ray data were collected on Bruker Smart APEX II CCD diffractometer. Bioimaging of the probes were performed on an Olympus FV1000 confocal microscopy and the excitation wavelength was set as 555 nm. The solvents and chemicals used for synthesis were commercially available from Aldrich and were of analytical-reagent grade. The solutions of metal ions were performed from their nitrate or chloride salts. Column flash chromatography was carried out on Merck silica gel (250–400 mesh ASTM). Thin-layer chromatography (TLC) was performed on silica gel GF254. Double distilled water was used throughout the experiment.

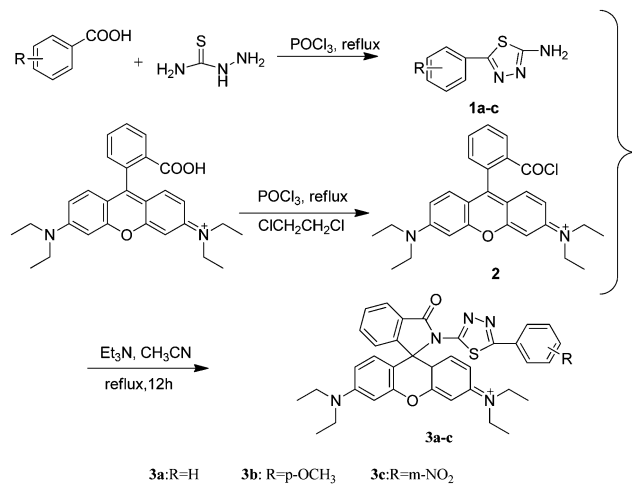
#### Synthesis of compounds 3a–c

Compounds 3a–c were readily prepared according to Scheme 1.

Compounds 1a–c were prepared according to the literature procedure.<sup>34</sup> Rhodamine B (1.59 g, 3 mmol) was dissolved in dry 1,2-dichloroethane (15 mL), followed by addition of phosphorus

Key Laboratory of Synthetic and Natural Functional Molecule Chemistry, Ministry of Education, College of Chemistry and Materials Science, Northwest University, Xi'an 710069, PR China. E-mail: yangbq@nwu.edu.cn; ymp1111@163.com; Fax: +86 29 88302617; Tel: +86 29 88302217

† Electronic supplementary information (ESI) available. CCDC 979338, 979341 and 979339. For ESI and crystallographic data in CIF or other electronic format see DOI: 10.1039/c4ra00396a



Scheme 1 Synthesis of 3a–c.

oxychloride (5 mL). After being heated to reflux for 4 h, the solvent and excess amount of phosphorus oxychloride was removed by evaporation to give the corresponding acid chloride, which was dissolved in acetonitrile without further purification. Then a solution of **1a** (0.59 g, 3 mmol), triethylamine (2 mL) in acetonitrile (20 mL) was added. After refluxing for 12 h, the solvent was removed under reduced pressure to give a violent-oil. Water was then added to the mixture and the aqueous was extracted with dichloromethane (15 mL × 3). The organic layer was dried over anhydrous MgSO<sub>4</sub> and filtered. The crude product was purified by silica gel column chromatography to give **3a** (white solid) in 71.2% yield. <sup>1</sup>H NMR (400 MHz, CDCl<sub>3</sub>) δ (ppm) 8.78 (s, 1H), 8.20 (dd, *J*<sub>1</sub> = 8.0, *J*<sub>2</sub> = 8.0 Hz, 2H), 8.09 (d, *J* = 8.0 Hz, 1H), 7.70–7.50 (m, 4H), 7.27 (d, *J* = 8.0 Hz, 1H), 6.50 (s, 2H), 6.39 (d, *J* = 8.0 Hz, 2H), 6.18 (d, *J* = 8.0 Hz, 2H), 3.30 (q, *J* = 4.0 Hz, 8H), 1.14 (t, *J* = 6.0 Hz, 12H). <sup>13</sup>C NMR (100 MHz, CDCl<sub>3</sub>) δ 165.83, 153.58, 153.40, 148.50, 134.24, 128.37, 128.21, 127.71, 127.27, 126.86, 124.46, 123.05, 106.78, 104.97, 97.49, 76.85, 76.53, 76.21, 68.03, 43.74, 12.18. HRMS (ESI) calcd for C<sub>36</sub>H<sub>35</sub>N<sub>5</sub>O<sub>2</sub>S [M + H]<sup>+</sup>: 602.2584, found: 602.2620.

Compounds **3b** and **3c** were prepared with the similar synthetic method to **3a**.

Compound **3b** (white solid): yield: 69.5%. <sup>1</sup>H NMR (400 MHz, CDCl<sub>3</sub>) δ (ppm) 8.06 (d, *J* = 7.5, 1H), 7.82 (d, *J* = 8.6, 2H), 7.62–7.53 (m, 2H), 7.29–7.17 (m, 1H), 6.89 (d, *J* = 8.7, 2H), 6.47 (d, *J* = 2.4, 2H), 6.39 (d, *J* = 8.8, 2H), 6.16 (dd, *J*<sub>1</sub> = 8.9, *J*<sub>2</sub> = 2.4, 2H), 3.81 (s, 3H), 3.29 (q, *J* = 7.0, 8H), 1.13 (t, *J* = 7.0, 12H). <sup>13</sup>C NMR (100 MHz, CDCl<sub>3</sub>) δ 165.75, 162.12, 160.66, 153.56, 153.40, 148.46, 134.19, 128.32, 128.19, 127.76, 127.29, 124.43, 123.02, 113.77, 106.73, 105.00, 97.45, 76.88, 76.56, 76.24, 67.92, 54.85, 43.74, 12.20. HRMS (ESI) calcd for C<sub>37</sub>H<sub>37</sub>N<sub>5</sub>O<sub>3</sub>S [M + H]<sup>+</sup>: 632.2690, found: 632.2714.

Compound **3c** (yellow solid): yield: 69.5%. <sup>1</sup>H NMR (400 MHz, CDCl<sub>3</sub>) δ (ppm) 8.07 (d, *J* = 8.0 Hz, 1H), 7.88 (d, *J* = 3.5 Hz, 2H), 7.63–7.54 (m, 2H), 7.25 (d, *J* = 7.9 Hz, 1H), 7.37 (s, 3H), 6.48 (d, *J* = 1.5 Hz, 2H), 6.39 (d, *J* = 8.8 Hz, 2H), 6.17 (d, *J* = 7.0 Hz, 2H), 3.30 (q, *J* = 8.0 Hz, 8H), 1.13 (t, *J* = 6.0 Hz, 12H). <sup>13</sup>C NMR (100 MHz, CDCl<sub>3</sub>) δ 160.69, 154.53, 149.71, 148.47, 148.06,

143.36, 142.87, 129.33, 127.09, 126.84, 124.27, 123.18, 122.13, 119.35, 118.76, 117.98, 116.35, 101.58, 99.45, 92.19, 71.66, 71.35, 71.03, 63.14, 47.77, 38.56, 6.98. HRMS (ESI) calcd for C<sub>36</sub>H<sub>34</sub>N<sub>6</sub>O<sub>4</sub>S [M + H]<sup>+</sup>: 632.2435, found: 632.2421.

### Preparation of the test solution

Rhodamine B based probes **3a–c** stock solutions (200 μM) were prepared in methanol. Stock solutions of metal ions were prepared with hydrochloride salts of Na<sup>+</sup>, K<sup>+</sup>, Ca<sup>2+</sup>, Cd<sup>2+</sup>, Mg<sup>2+</sup>, Co<sup>2+</sup>, Mn<sup>2+</sup>, Cu<sup>2+</sup>, Al<sup>3+</sup>, Zn<sup>2+</sup>, Ni<sup>2+</sup>, Fe<sup>2+</sup>, Hg<sup>2+</sup>, Cr<sup>3+</sup>, Fe<sup>3+</sup>, and the nitrate salt of Ag<sup>+</sup> in distilled water. Before spectroscopic measurements, the solutions of **3a–c** were freshly prepared by diluting the high concentration stock solution to corresponding solution. All the measurements were made according to the following procedure. Test solutions were prepared by placing 1 mL of the probe solution into a glass tube, adding an appropriate aliquot of each metal stock, and diluting the solution to 10 mL with methanol–water (4/6, v/v) solution. To make the metal ions chelate with the probe sufficiently, solutions were shaken for 10 s and waited for 20 min before determination. The absorbance was recorded at 562 nm and the fluorescence intensity was recorded at 583 nm. The excitation and emission wavelength bandpasses were both set as 2.5 nm and the excitation wavelength was set at 555 nm.

### Cell culture and fluorescence imaging

The human cancer cell line HepG2 (liver cells) were cultured in RPMI 1640 supplemented with 10% FBS. Immediately before the experiments, cells were pretreated with probes **3a–c** (20 μM) for 1 h at 37 °C in humidified air and 5% CO<sub>2</sub>, washed three times with PBS and imaged. After incubation with FeCl<sub>3</sub> (20 μM) for another 1.5 h at 37 °C, cells were washed 3 times with PBS to remove remaining FeCl<sub>3</sub> and imaged.

## Results and discussion

### Synthesis and crystal structure

The general synthetic procedure is given in Scheme 1. The target compound **3a** was easily synthesized by the reaction of rhodamine B acid chloride (**2**) and **1a**. Title compounds **3b** and **3c** were also prepared by similar procedures. The structures of compounds **3a–c** were characterized by <sup>1</sup>H NMR, <sup>13</sup>C NMR, and HRMS analyses. Crystals of compounds **3a–c** were obtained from a mixture of methanol–dichloromethane. In Fig. 1, a unique spiro lactam structure ring formation of **3a** was observed (the crystal data of **3a–c** are shown in ESI†).

### Spectroscopic properties

Upon binding with Fe<sup>3+</sup>, the probes **3a–c** exhibited similar spectroscopic properties. The R moiety had an effect on the fluorescence intensities of the probes. However, no obvious effects were found to be caused by the R moiety on the other spectral properties of the probes. Thus, **3a** is chosen for further discussion, optical spectra of **3b** and **3c** are shown in the ESI.†

The UV-vis titration of the probe **3a** was carried out in methanol–water (4/6, v/v) solution (Fig. 2a). Initially, free probe

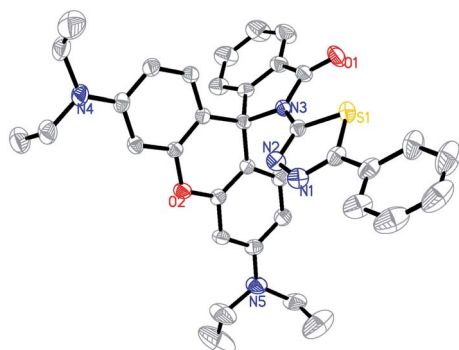


Fig. 1 X-ray crystal structure of **3a**.

**3a** displayed almost no absorption above 500 nm, which indicated that the spiroactam form was presented predominantly. Addition of  $\text{Fe}^{3+}$  into solution immediately resulted in a significant enhancement of absorbance at about 562 nm. This

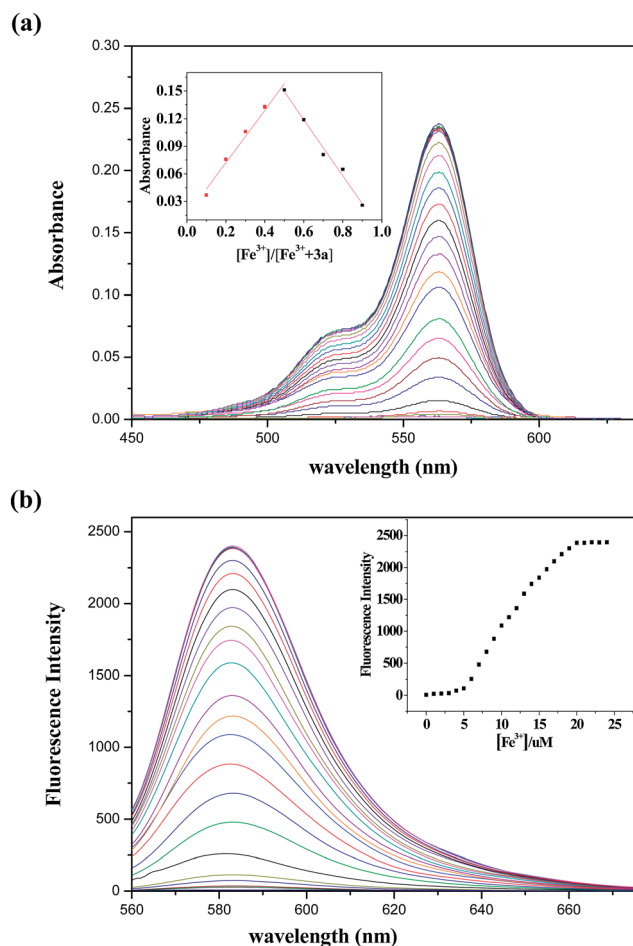


Fig. 2 (a) Changes in UV-vis absorption spectra of **3a** (20  $\mu\text{M}$ ) with various amounts of  $\text{Fe}^{3+}$  in methanol–water (4/6, v/v) solution. Inset: Job's plot of **3a** and  $\text{Fe}^{3+}$ . The total concentration was 20  $\mu\text{M}$ . (b) Changes in fluorescence spectra of **3a** (20  $\mu\text{M}$ ) with various amounts of  $\text{Fe}^{3+}$  in methanol–water (4/6, v/v) solution. Inset: changes in the emission intensity at 583 nm.

suggested the opening of the closed rhodamine–spiroactam ring. The titration curve showed that the increase was saturated with more than 1.0 equiv. of  $\text{Fe}^{3+}$ . Binding analysis using the job's method of continuous variations (Job's plot) indicated a 1 : 1 stoichiometry between **3a** and  $\text{Fe}^{3+}$  (Fig. 2a, inset). Moreover, the titration solution exhibited an obvious and characteristic color change from colorless to red. The above results implied that **3a** could serve as a “naked-eye” probe for  $\text{Fe}^{3+}$ .

In order to further investigate the interaction of **3a** and  $\text{Fe}^{3+}$ , a fluorescence titration experiment was carried out. Upon gradual addition of  $\text{Fe}^{3+}$ , the fluorescence intensity of **3a** increased at 583 nm (Fig. 2b). After adding 1.0 equiv. of  $\text{Fe}^{3+}$ , the fluorescence intensity showed negligible changes (Fig. 2b, inset). The association constants  $K$  of probes with  $\text{Fe}^{3+}$  were estimated by the Benesi–Hildebrand equation:  $(F_{\text{max}} - F_0)/(F_x - F_0) = 1 + (1/K)(1/[M]^n)$ , where  $F_{\text{max}}$ ,  $F_0$ , and  $F_x$  are fluorescence intensities of probe in the presence of  $\text{Fe}^{3+}$  at saturation, free probe, and any intermediate  $\text{Fe}^{3+}$  concentration (Fig. S4, ESI<sup>†</sup>). Based on the assumption of 1 : 1 binding model ( $n = 1$ ), the results obtained were  $K_{3a} = 3.24 \times 10^4 \text{ M}^{-1}$ ,  $K_{3b} = 2.52 \times 10^4 \text{ M}^{-1}$  and  $K_{3c} = 3.01 \times 10^4 \text{ M}^{-1}$ . The fluorescence quantum yields ( $\Phi$ ) were determined by using rhodamine B ( $\Phi_s = 0.97$  in ethanol) as standards and the quantum yields were calculated using equation:  $\Phi_u = \Phi_s(A_s/A_u)(I_u/I_s)(\eta_u/\eta_s)$ , where  $\Phi_u$  and  $\Phi_s$  are the fluorescence quantum yields,  $A_u$  and  $A_s$  are the absorbance,  $I_u$  and  $I_s$  are the integrated emission intensities of the corrected spectra, and  $\eta_u$  and  $\eta_s$  are the indices of refraction of the sample and standard solutions, respectively. Based on the equation, the results obtained were  $\Phi_{3a} = 0.32$ ,  $\Phi_{3b} = 0.30$ ,  $\Phi_{3c} = 0.38$ . To study the stability of the complex formed, we also have analyzed the chemical reversibility behavior of the binding of **3a** and  $\text{Fe}^{3+}$ . Upon addition of ethylenediamine to the mixture of **3a** (20  $\mu\text{M}$ ) and  $\text{Fe}^{3+}$  (20  $\mu\text{M}$ ), the color of the mixture changed back to colorless, and fluorescent intensity decreased (Fig. 3). These findings suggested that **3a** is a reversible fluorescent probe toward  $\text{Fe}^{3+}$ .

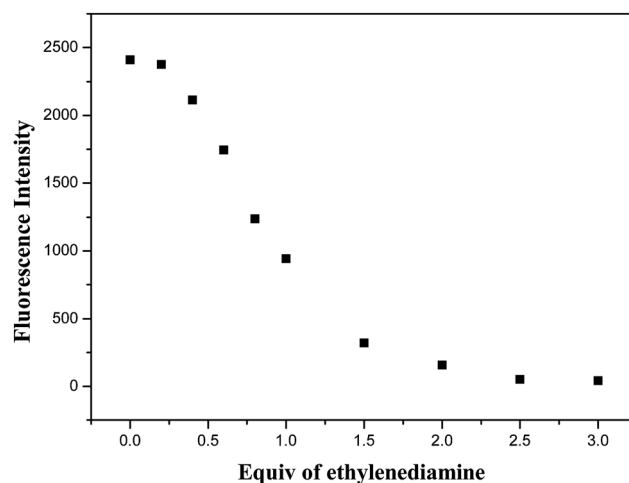


Fig. 3 Fluorescence intensity changes of **3a** (20  $\mu\text{M}$ ) upon the addition of each equiv. of ethylenediamine with the presence of  $\text{Fe}^{3+}$  (20  $\mu\text{M}$ ) in methanol–water (4/6, v/v) solution.

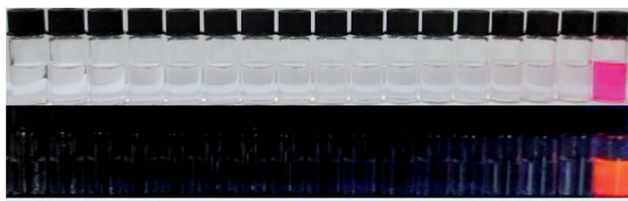


Fig. 4 Pictures of **3a** as a selective naked-eye probe (top) and the visual fluorescence emissions by using a UV lamp (365 nm) (bottom) for  $\text{Fe}^{3+}$ . From the left to right: blank,  $\text{Ag}^+$ ,  $\text{Na}^+$ ,  $\text{K}^+$ ,  $\text{Ca}^{2+}$ ,  $\text{Cd}^{2+}$ ,  $\text{Mg}^{2+}$ ,  $\text{Co}^{2+}$ ,  $\text{Mn}^{2+}$ ,  $\text{Cu}^{2+}$ ,  $\text{Al}^{3+}$ ,  $\text{Zn}^{2+}$ ,  $\text{Ni}^{2+}$ ,  $\text{Fe}^{2+}$ ,  $\text{Hg}^{2+}$ ,  $\text{Cr}^{3+}$  and  $\text{Fe}^{3+}$  ions.

High selectivity is a very important parameter to evaluate the performance of a probe. We examined the fluorescent and UV-vis spectra of probe **3a** response to different metal ions, including  $\text{Na}^+$ ,  $\text{K}^+$ ,  $\text{Ca}^{2+}$ ,  $\text{Cd}^{2+}$ ,  $\text{Mg}^{2+}$ ,  $\text{Co}^{2+}$ ,  $\text{Mn}^{2+}$ ,  $\text{Cu}^{2+}$ ,  $\text{Al}^{3+}$ ,  $\text{Zn}^{2+}$ ,  $\text{Ni}^{2+}$ ,  $\text{Fe}^{2+}$ ,  $\text{Hg}^{2+}$ ,  $\text{Cr}^{3+}$ ,  $\text{Ag}^+$  and  $\text{Fe}^{3+}$ . Among the various metal ions examined, a significant enhancement of the fluorescence with color changes of **3a** emerged soon after  $\text{Fe}^{3+}$  was added. However, other metal ions did not induce any spectral response (Fig. 4 and S5<sup>†</sup>). The competitive experiments were conducted by adding  $\text{Fe}^{3+}$  to probe **3a** solution in the presence of other metal ions. As a result, the  $\text{Fe}^{3+}$ -induced spectral enhancement was not affected by the tested background metal ions (Fig. 5). Selectivity and competition experiments indicated that probe **3a** is selective and sensitive for the detection of  $\text{Fe}^{3+}$ .

To further confirm why the significant absorbance and fluorescence of **3a** changed, the IR spectra experiments were carried out. IR spectra of **3a** and **3a-Fe**<sup>3+</sup> were taken in KBr disks, respectively. As demonstrated in Fig. 6, the carbonyl absorption of **3a** at  $1705.00\text{ cm}^{-1}$  disappeared upon the addition of  $\text{Fe}^{3+}$ . This supports that carbonyl oxygen is actually

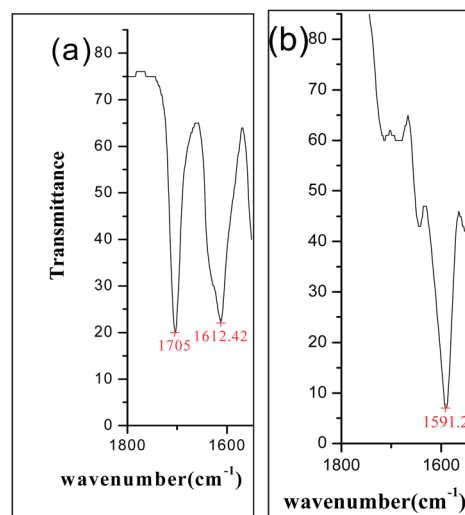
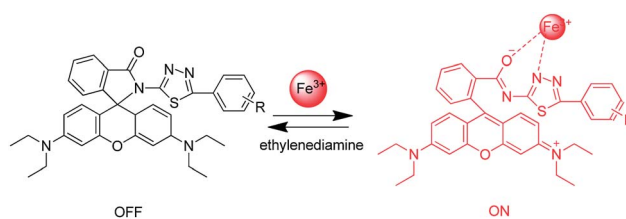


Fig. 6 IR spectra of **3a** (a) and **3a** +  $\text{Fe}^{3+}$  (b).



Scheme 2 Proposed mechanism for the fluorescent changes of probes upon the addition of  $\text{Fe}^{3+}$ .

involved in the coordination with  $\text{Fe}^{3+}$ . Thus, the most possible binding sites for  $\text{Fe}^{3+}$  are the conjugated moieties including O and N atoms (Scheme 2). It is very likely due to the chelation-induced ring opening of rhodamine spirolactam, rather than other possible reactions.

### Fluorescence imaging

In order to further evaluate the potential of the probes for imaging  $\text{Fe}^{3+}$  in living cells, cultured HepG2 cells were incubated with the probes for 1 h at  $37\text{ }^\circ\text{C}$ . The cells incubated with only probes ( $20\text{ }\mu\text{M}$ ) exhibited almost no fluorescence (Fig. 7a). By contrast, the cells stained with both the probe and further incubated with  $\text{FeCl}_3$  ( $20\text{ }\mu\text{M}$ ) displayed bright red fluorescence (Fig. 7b). Bright-field transmission images of cells treated with  $\text{FeCl}_3$  and probe revealed that the cells were viable throughout the imaging experiments (Fig. 7c). Taken together, these results demonstrate that probes **3a-c** are cell membrane-permeable and effective intracellular imaging agent for  $\text{Fe}^{3+}$  ions.

## Conclusions

In summary, we have synthesized three new rhodamine-based probes **3a-c**, which can give highly selective and sensitive

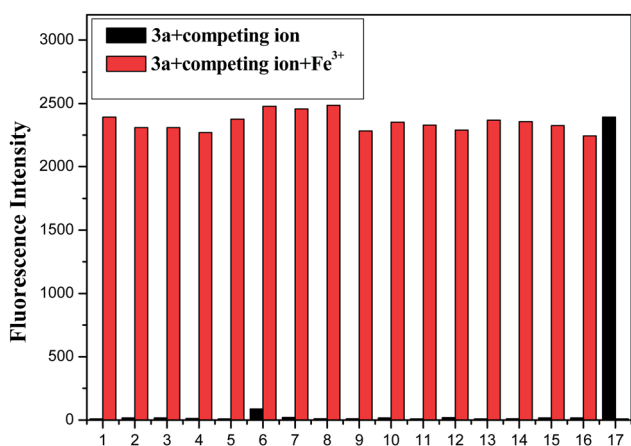


Fig. 5 Fluorescence intensity changes of **3a** ( $20\text{ }\mu\text{M}$ ) upon the addition of various metal ions ( $20\text{ }\mu\text{M}$ ) in and without the presence of  $\text{Fe}^{3+}$  ( $20\text{ }\mu\text{M}$ ) in methanol–water (4/6, v/v) solution. The black bars represent the fluorescence response of **3a** and competing ions: (1) blank, (2)  $\text{Na}^+$ , (3)  $\text{Ca}^{2+}$ , (4)  $\text{Mg}^{2+}$ , (5)  $\text{Cd}^{2+}$ , (6)  $\text{Mn}^{2+}$ , (7)  $\text{Ni}^{2+}$ , (8)  $\text{Co}^{2+}$ , (9)  $\text{Zn}^{2+}$ , (10)  $\text{Cu}^{2+}$ , (11)  $\text{Cr}^{3+}$ , (12)  $\text{Pb}^{2+}$ , (13)  $\text{Ag}^+$ , (14)  $\text{Fe}^{2+}$ , (15)  $\text{Hg}^{2+}$ , (16)  $\text{K}^+$  and (17)  $\text{Fe}^{3+}$ . The red bars represent the subsequent addition of  $20\text{ }\mu\text{M}$   $\text{Fe}^{3+}$  to the above solutions.

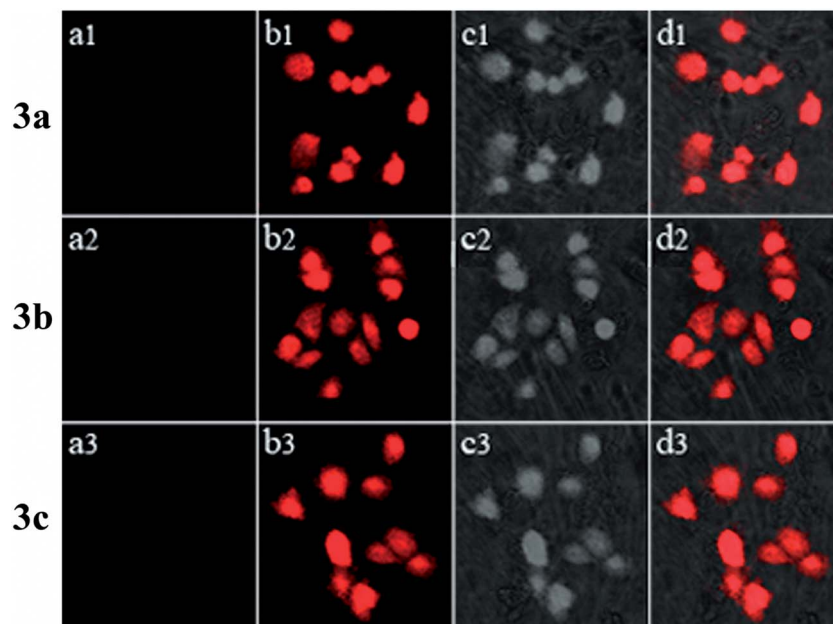


Fig. 7 Bioimaging application of probes in HepG2 cells. Representative fluorescence images of HepG2 cells treated with probes (20  $\mu\text{M}$ ) in either the absence (a) or the presence (c) of 20  $\mu\text{M}$   $\text{Fe}^{3+}$  for 1 h at 37  $^{\circ}\text{C}$ . (b) Bright-field image of cells shown in panel. (d) Overlay image of (b) and (c).

responses to  $\text{Fe}^{3+}$ . Iron specific binding enabled the opening of the spiro lactam ring and consequently successfully exhibited absorption and fluorescence enhancement response toward  $\text{Fe}^{3+}$  ions over other metal ions (even those exist in high concentration). The probes were successfully applied to the microscopic imaging for detection of  $\text{Fe}^{3+}$  in HepG2 cells with fluorescent methods.

## Acknowledgements

This work was supported by the National Natural Science Foundation of China (no. 21172178).

## Notes and references

- 1 B. D' Autréaux, N. P. Tucker, R. Dixon and S. Spiro, *Nature*, 2005, **437**, 769.
- 2 J. W. Lee and J. D. Helmann, *Nature*, 2006, **440**, 363.
- 3 M. Ghaedi, A. Shokrollahi, R. Mehrnoosh, O. Hossaini and M. Soylak, *Cent. Eur. J. Chem.*, 2008, **6**, 488.
- 4 E. Beutler, V. Felitti, T. Gelbart and N. Ho, *Drug Metab. Dispos.*, 2001, **29**, 495.
- 5 C. Brugnara, *Clin. Chem.*, 2003, **49**, 1573.
- 6 R. R. Crichton, D. T. Dexter and R. J. Ward, *Coord. Chem. Rev.*, 2008, **252**, 1189.
- 7 J. R. Burdo and J. R. Connor, *BioMetals*, 2003, **16**, 63.
- 8 D. J. Bonda, H. Lee, J. A. Blair, X. Zhu, G. Perry and M. A. Smith, *Metallomics*, 2011, **3**, 267.
- 9 A. S. Pithadia and M. H. Lim, *Curr. Opin. Chem. Biol.*, 2012, **16**, 67.
- 10 J. Zhang, C. W. Yu, S. Y. Qian, G. Lu and J. W. Chen, *Dyes Pigm.*, 2012, **92**, 1370.
- 11 S. X. Wang, X. M. Meng and M. Z. Zhu, *Tetrahedron Lett.*, 2011, **52**, 2840.
- 12 Q. J. Ma, X. B. Zhang, X. H. Zhao, Z. Jin, G. J. Mao, G. L. Shen and R. Q. Yu, *Anal. Chim. Acta*, 2010, **663**, 85.
- 13 X. F. Yang, M. L. Zhao and G. Wang, *Sens. Actuators, B*, 2011, **151**, 8.
- 14 H. Kim, S. Lee, J. Lee and J. Tae, *Org. Lett.*, 2010, **12**, 5342.
- 15 W. Y. Lin, X. W. Cao, Y. D. Ding, L. Yuan and L. L. Long, *Chem. Commun.*, 2010, **46**, 3529.
- 16 J. F. Zhang, Y. Zhou, J. Yoon, Y. Kim, S. J. Kim and J. S. Kim, *Org. Lett.*, 2010, **12**, 3852.
- 17 M. Kumar, N. Kumar, V. Bhalla, H. Singh, P. R. Sharma and T. Kaur, *Org. Lett.*, 2011, **13**, 1422.
- 18 M. H. Lee, T. V. Giap, S. H. Kim, Y. H. Lee, C. Kang and J. S. Kim, *Chem. Commun.*, 2010, **46**, 1407.
- 19 Q. A. Best, R. S. Xu, M. E. McCarroll, L. C. Wang and D. J. Dyer, *Org. Lett.*, 2010, **12**, 3219.
- 20 X. Y. Hu, J. Wang, X. Zhu, D. P. Dong, X. L. Zhang, S. Wu and C. Y. Duan, *Chem. Commun.*, 2011, **47**, 11507.
- 21 W. Lin, L. Long, L. Yuan, Z. Cao and J. Feng, *Anal. Chim. Acta*, 2009, **634**, 262.
- 22 Y. Xiang and A. Tong, *Org. Lett.*, 2006, **8**, 1549.
- 23 L. Dong, C. Wu, X. Zeng, L. Mu, S. F. Xue, Z. Tao and J. X. Zhang, *Sens. Actuators, B*, 2010, **145**, 433.
- 24 W. Yin, H. Cui, Z. Yang, C. Li, M. She, B. Yin, J. Li, G. Zhao and Z. Shi, *Sens. Actuators, B*, 2011, **157**, 675.
- 25 Z. Yang, M. She, B. Yin, J. Cui, Y. Zhang, W. Sun, J. Li and Z. Shi, *J. Org. Chem.*, 2012, **77**, 1143.

- 26 J. Mao, L. Wang, W. Dou, X. Tang, Y. Yan and W. Liu, *Org. Lett.*, 2007, **9**, 4567.
- 27 N. C. Lim, S. V. Pavlova and C. Brückner, *Inorg. Chem.*, 2009, **48**, 1173.
- 28 J. P. Sumner and R. Kopelman, *Analyst*, 2005, **130**, 528.
- 29 X. Zhang, Y. Shiraishi and T. Hirai, *Tetrahedron Lett.*, 2007, **48**, 5455.
- 30 C. Wolf, X. Mei and H. K. Rokadia, *Tetrahedron Lett.*, 2004, **45**, 7867.
- 31 J. L. Bricks, A. Kovalchuk, C. Trieflinger, M. Nofz, M. Büschel, A. I. Tolmachev, J. Daub and K. Rurack, *J. Am. Chem. Soc.*, 2005, **127**, 13522.
- 32 Y. Ma, W. Luo, P. J. Quinn, Z. Liu and R. C. Hider, *J. Med. Chem.*, 2004, **47**, 6349.
- 33 X. Wu, B. Xu, H. Tong and L. Wang, *Macromolecules*, 2010, **43**, 8917.
- 34 P. Guan, F. Sun, X. Hou, F. Wang, F. Yi, W. Xu and H. Fang, *Bioorg. Med. Chem.*, 2012, **20**, 3865.